THE JOURNAL OF PHYSICAL CHEMISTRY C

Article

pubs.acs.org/JPCC

Luminescence and Raman Detection of Molecular Cl_2 and ClClO Molecules in Amorphous SiO_2 Matrix

Linards Skuja,*[,†] Koichi Kajihara,[‡] Krisjanis Smits,[†] Andrejs Silins,[†] and Hideo Hosono[§]

[†]Institute of Solid State Physics, University of Latvia, 8 Kengaraga street, LV1063, Riga, Latvia

[‡]Department of Applied Chemistry, Graduate School of Urban Environmental Sciences, Tokyo Metropolitan University, 1-1 Minami-Osawa, Hachioji, Tokyo 192-0397, Japan

[§]Laboratory for Materials and Structures & Materials Research Center for Element Strategy, Tokyo Institute of Technology, 4259 Nagatsuta, Midori-ku, Yokohama 226-8503, Japan

ABSTRACT: Chlorine is a common undesirable impurity in synthetic SiO_2 glass for ultraviolet optics and optical fibers. It is usually incorporated into glass as bound Si−Cl groups or interstitial Cl_2 molecules. We report a high-sensitivity detection of Cl_2 in amorphous SiO_2 (a-SiO_2) by photoluminescence (PL) and also by Raman spectroscopy. The Cl_2 PL emission band at 1.22 eV (1016 nm) appears at T < 160 K and shows a characteristic vibronic progression with separations ≈(520−540) cm^{-1} and an average lifetime of ≈5 ms at 13 K. Its excitation spectrum coincides with the shape of the 3.78 eV (328 nm) optical absorption band of Cl_2 in a-SiO_2, corresponding to the X → A $^1\Pi_u$ transition to repulsive excited state. Direct X → a singlet-to-triplet excitation was also observed at 2.33 eV (532 nm). Cl_2 PL may serve as a sensitive and selective tool for monitoring Cl impurities and their reactions in a-SiO_2. A Raman band of Cl_2 is found at 546 cm^{-1}. Cl_2 photodissociation at energies up to 4.66 eV (266 nm) was not detected, pointing to a strong cage effect in a-SiO_2 matrix. However, 7.9 eV (157 nm) photolysis of interstitial O_2 molecules gives rise to a Raman band at 954 cm^{-1}, indicating a formation of dichlorine monoxide isomer, ClClO molecule by reaction of O atoms with interstitial Cl_2.

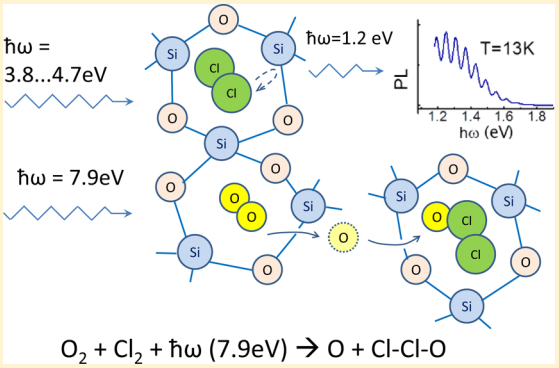

INTRODUCTION

Synthetic amorphous SiO_2 ("a-SiO_2") is widely used in optics, photonics, chemical, nuclear, and space technologies. Although often referred as "high purity", in most cases it contains significant (10^{15}−10^{18} cm^{-3}) amount of chlorine impurities, left after manufacturing by oxidation of $SiCl_4$, or from usage of Cl_2 atmosphere to remove Si−OH impurities in low−OH "dry" silicas. The presence of Cl is detrimental for applications requiring deep-ultraviolet (DUV) and vacuum UV (VUV) transparency,[1] resistance against solarization caused by UV-light and/or stability of optical properties in nuclear or space radiation environments.[2] a-SiO_2 with improved VUV transparency is obtained in chlorine-free processes: sol−gel technique,[3] or industrially, by substituting $SiCl_4$ as a raw material by organic siloxanes, e.g., octamethylcyclotetrasiloxane (OMCTS).[4] Cl impurities are incorporated mostly as chloride (≡Si−Cl) groups, where the Si atom is bounded through 3 "bridging" oxygens to the rest of a-SiO_2 network. A smaller fraction of Cl impurities forms interstitial Cl_2 molecules. The presence of excess oxygen in a-SiO_2 network increases the relative fraction of Cl_2 vs Si−Cl groups, while in the presence of interstitial H_2 chlorine tends to form interstitial HCl molecules.[5]

Chlorine impurities in a-SiO_2 are hard to monitor by spectroscopic methods. Si−Cl groups have no optical absorption (OA) bands in the visible-to-DUV range and only cause an additional unstructured absorption near the VUV fundamental absorption edge.[1] Infrared absorption/Raman band of ≡Si−Cl bond stretching mode at ≈620 cm^{-1}[6] is typically too weak to be resolved on the background of the fundamental bands. Raman band of Cl_2 in SiO_2 has not been reported. However, in contrast to Si−Cl groups, interstitial Cl_2 molecules in a-SiO_2 have a distinct OA band at 3.8 eV (326 nm)[1] corresponding to the X $^1\sum_g^+$ → A $^1\Pi_{1u}$ band in a free Cl_2 molecule. However, its absorption peak cross section ($\sigma = 2.6 \times 10^{-19}$ cm^2 for free Cl_2[7]) is low in comparison with other OA bands in irradiated a-SiO_2. It is often obscured by the wing of the broad OA band at 4.8 eV (258 nm) due to dangling oxygen bonds;[8] moreover, it can be confused with the OA band at 3.7 eV (335 nm) due to the singlet-to-triplet transition in a divalent Ge atom[9] in Ge-doped a-SiO_2.

A weak PL emission in the 1.5 eV (≈800 nm) region showing vibrational structures was found in a-SiO_2[10] and tentatively assigned to ≡Si−O−O−Si≡ (peroxide linkage) bonding configuration.[11] Subsequently it was noted[12] that the reported[10,11] PL bears resemblance to the PL of Cl_2 in inert gas

Received: December 30, 2016
Revised: February 9, 2017
Published: February 10, 2017

DOI: 10.1021/acs.jpcc.6b13095
J. Phys. Chem. C 2017, 121, 5261−5266

Table 1. Sample Characterization

sample	3.8 eV (157 nm) OA band (cm^{-1})	$[Cl_2]$ (mol./cm^3)	$[O_2]$ (mol./cm^3)	$[\equiv Si-O-H]$ (groups/cm^3)	7.9 eV (157 nm) irradiation (photons/cm^2)
"S2" (high Cl_2, irradiated)	0.204	7.9×10^{17}	4.3×10^{17}	5.3×10^{16}	9.2×10^{19}
"S1" (high Cl_2, pristine)	0.171	6.6×10^{17}	2.9×10^{17}	5.7×10^{16}	not irradiated
"S0" (low Cl_2, pristine)	0.018	5.4×10^{16}	2.8×10^{17}	1.2×10^{17}	not irradiated

matrices;[13] however, it was not further explored. Due the advances in sensitive near-IR light detectors, this spectral region has become more accessible. Here we report detailed properties of the PL of interstitial Cl_2 in a-SiO_2 and show that it can serve as a sensitive tool to monitor the concentration of interstitial Cl_2. The Raman signal of interstitial Cl_2 is identified as well. It is shown that Cl_2 in SiO_2 is stabilized against photolysis by the cage effect, and that Cl_2 reacts with mobile O atom to form an isomer of dichlorine monoxide, the ClClO molecule.

EXPERIMENTAL SECTION

Three synthetic a-SiO_2 samples denoted S0, S1, and S2, optically polished, sized $5 \times 10 \times 12$ mm^3, and manufactured by oxidizing $SiCl_4$ in oxygen plasma were investigated. Samples S1 and S2 are distinguished from S0 by >10 times higher concentration of trapped Cl_2 molecules, while concentrations of trapped O_2 and bound silanol groups in all samples are comparable within a factor of 2 (Table 1). Additionally, S2 was irradiated by F_2 laser (7.9 eV/157 nm, 116 J/cm^2, T = 300 K). Cl_2 concentrations $[Cl_2]$ were determined from the amplitudes of the Cl_2 3.8 eV (326 nm) optical absorption (OA) band using peak cross section $\sigma = 2.58 \times 10^{-19}$ cm^2.[7] $[O_2]$ was calculated from infrared PL/Raman spectra as described in ref 5. [Si−OH] was obtained from the 3700 cm^{-1} infrared OA band using $\sigma = 3.14 \times 10^{-19}$ cm^2.[14] For each species, the accuracy of the relative concentrations (concentration ratios) is ±5%, while the absolute concentrations are less accurate (±25%) due to uncertainties in the respective calibration coefficients.[5,7,14]

The optical absorption was measured at T = 295 K (Hitachi U4000), the PL and PL excitation (PLE) spectra and PL decay kinetics were measured in the T range 14−300 K in a He refrigerator cryostat (Leybold RDK 10−320). PL was excited at several wavelengths by diode-pumped solid state lasers with photon energies (wavelengths) 2.33 eV (532 nm), 2.62 eV (473 nm), and 4.66 eV (266 nm); by a GaN diode laser (3.31 eV/374 nm); and by a N_2 gas laser (3.68 eV/337 nm). The PL and Raman spectra were recorded by 300 mm Andor Shamrock spectrograph (150 L/mm grating PL, 1200 L/mm Raman) and cooled CCD camera (Andor DU971N-UVB). The artifacts, caused by interference fringes (etaloning) in the back-illuminated CCD in the near IR spectral region were removed by calibrating against the spectrum of a standard tungsten lamp. The PL spectral resolution was 5 meV in the 1.2−1.7 eV region. PLE spectra were measured using a 150 W Xe-lamp filtered by 200 mm double monochromator (AMKO LTI). The wavelength-dependence of the excitation intensity was measured by comparing to standard deuterium lamp (Ocean Optics DH-2000-CAL). PL kinetics was obtained by mechanically chopping the excitation light and recording the integral PL signal between 1.55 and 2.1 eV with photomultiplier (Hamamatsu R955) and multichannel photon counter. Decay curve fitting was done using MATLAB optimization toolbox.

Raman spectra were collected with a purpose-built system in the common backscattering geometry, using Nd:YAG laser (LSR532H, λ = 532.09 nm, 400 mW), a condenser with antireflection coated f/1.6 silica lenses, a laser line cleanup filter, a dichroic 45° mirror, and a long pass edge filter (Semrock LL01-532, LPD01-532, and LP03-532, respectively). Spectral resolution was 6 cm^{-1} (full width at half-maximum, fwhm), wavenumber accuracy 1 cm^{-1}. The purpose of the measurement was to obtain minor (≈0.1%) differences in Raman spectra of samples S2 and S0 with different Cl_2 concentrations. This level of accuracy requires: (i) a low noise level, (ii) a low intensity drift, and (iii) an absence of CCD-related small artifacts ("built-in" pixel noise). To accomplish this: (i) 600 nearly full-scale 16 bit spectra were averaged at each measurement (≈1.7×10^7 ADC counts per pixel bin), (ii) three pairs of thus averaged spectra were taken alternatively reinserting samples S0 and S2 to check the intensity drift and repeatability, and (iii) an additional three pairs of similarly averaged spectra were measured with the spectrograph center point shifted by 1.5 nm to verify that the influence of CCD pixel nonuniformity was negligible.

RESULTS

The PL emission spectra of Cl-containing a-SiO_2 sample S1 are shown in Figure 1. A broad luminescence emerges at

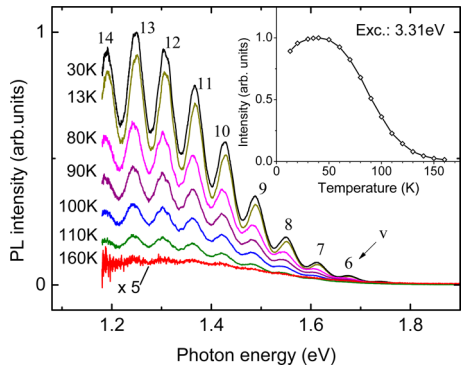

Figure 1. Photoluminescence spectra of Cl_2-containing amorphous SiO_2 (sample S1) measured at 3.31 eV (374 nm) CW laser excitation (2 mW) at temperatures between 13 and 160 K. Inset shows the temperature dependence of intensity, integrated over the 1.2−1.8 eV (1033 nm-689 nm) region. Numbering of sub-bands indicates the ground state vibrational level quantum numbers v of Cl_2 molecule.

temperatures T < 160 K. Distinct vibronic structures develop at T < 110 K, showing series of narrow sub-bands with fwhm ≈30 meV and separations decreasing from 65 meV at 1.8 eV to 58 meV at 1.2 eV. The smaller structures visible in some subbands are artifacts due to incompletely corrected etaloning of CCD.

A Gaussian fit to the broad-band component of PL yields peak at 1.22 eV (1016 nm) and fwhm of 0.42 eV. This PL was observed at all discrete laser photon energies used (2.33, 2.62, 3.31, 3.68, 4.66 eV). The excitation peak is at 3.80 eV (326 nm) with fwhm =0.6 eV (Figure 2B); it nearly coincides with the

DOI: 10.1021/acs.jpcc.6b13095
J. Phys. Chem. C 2017, 121, 5261−5266

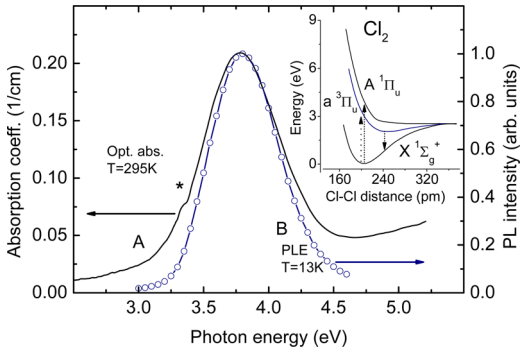

Figure 2. (A) Optical absorption spectrum, measured at 295 K (sample S2, before irradiation). The feature marked by an asterisk is an instrument artifact. (B) Photoluminescence excitation spectrum, (sample S1, T = 14 K, resolution 0.05 eV). The inset shows potential energy curves for the ground (X) and the lowest excited states (a and A) of Cl_2 molecule, calculated in ref 15; arrows indicate the observed excitation and luminescence transitions.

absorption spectrum (Figure 2A). The emission spectra taken using different energies within this excitation band preserved the same form; no peak shifts could be detected. The intensity of the 1.22 eV PL band under UV laser excitation (3.31 eV, 4.66 eV) remained constant (±1%) under prolonged (1 h) irradiation, photobleaching was not detected.

High-intensity (50 mW) excitation at photon energy 2.32 eV, much below the energies of the PLE band of Figure 2, produced a weak infrared PL band, overlapped by the wing of the PL band due to oxygen dangling bonds "non-bridging oxygen hole centers" (NBOHC)[16] (Figure 3). It shows the same characteristic vibronic structure as present in Figure 1.

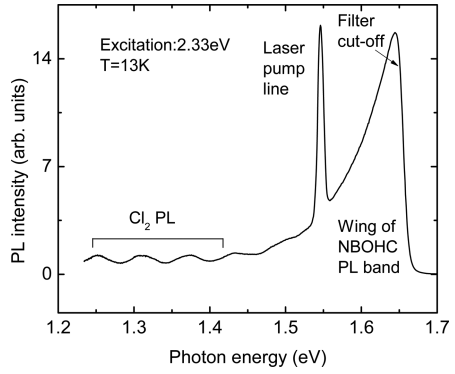

Figure 3. Infrared luminescence of Cl_2 molecules in SiO_2 (sample S1) under direct excitation to the radiative $^3\Pi_u$ state (see the inset to Figure 2), overlapped by a wing of 1.9 eV PL band due to oxygen dangling bonds (NBOHC's).

The PL decay kinetics (Figure 4) deviates from the single-exponent law when measured over dynamic range of 3 decades. At least 3 exponents with different decay constants τ_i had to be included in the nonlinear least-squares fit $I(t) = \sum_{i=1}^{3} C_i \exp(-t/\tau_i)$ to obtain a fair agreement with the data. The quality of the fit was not improved by inclusion of additional exponents. Fitting with a stretched exponent function $I(t) = Ce^{-[t+t_0/\tau]^{\beta}}$ gave significantly worse results. An excellent fit to kinetics, measured at 13 K (Figure 4, top curve) was obtained with decay constants 3.04, 7.28, and 16.67 ms (Figure 4, red line). Their relative contributions $\tau_i \times C_i$ to the total intensity

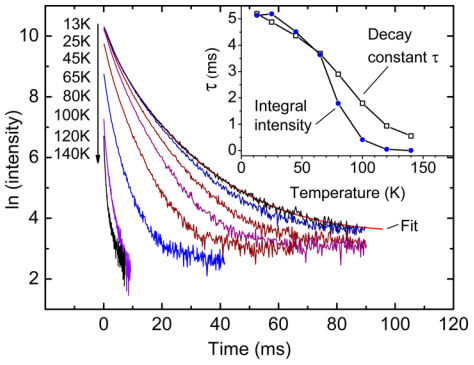

Figure 4. Luminescence decay kinetics measured for the spectral range 1.55−1.7 eV (800−729 nm) at temperatures between T = 13 and 140 K with 2.62 eV (473 nm) excitation (sample S1). The smooth red line shows a three-exponent fit to the kinetics at T = 13 K. Inset shows the temperature dependences of the normalized luminescence intensity (filled circles) and of the average decay constant τ, obtained by least-squares fitting to a single exponent (hollow squares).

were 34.4%. 50.3%, and 15.3%, respectively. While obviously not unique, this fit gives a rough outline of the underlying, probably continuous, distribution of τ. The T-dependence of the "average" τ was estimated, using a nonlinear fit with a single exponent. The average τ is ≈5.2 ms at 13 K; it decreases to 0.6 ms at 140 K (Figure 4, inset). The τ value at 20 K is 5 ms, ≈2.5 times larger than previously reported.[10]

The Figure 5 bottom trace shows the nearly coinciding Raman spectra of "low-Cl_2" sample S0 and "high-Cl_2" F_2-laser

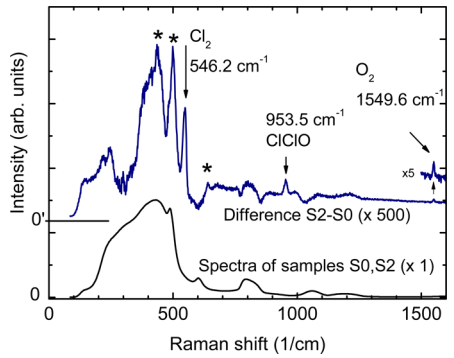

Figure 5. Raman spectra of Cl_2 and ClClO molecules in amorphous SiO_2. Bottom trace(s): two overlapping Raman spectra of the "low-Cl_2", unirradiated sample S0, and of the "high-Cl_2", F_2-laser-irradiated sample S2. Top trace: the difference spectrum S2 − S0 (×500). Peaks due to interstitial Cl_2, ClClO and O_2 molecules are marked by arrows. Peaks marked by asterisks may be subtraction-induced artifacts; their spectral positions were unstable against small deviations in the intensity of S0 relative to S2.

irradiated sample S2. They have the usual shape of the fundamental Raman spectrum of a-SiO_2. Top trace shows the difference spectrum S2 − S0 multiplied by 500, obtained as average of six pairs of sequentially measured spectra of samples S0, S2 (see the Experimental Section). The difference spectra, obtained individually from each of these 6 pairs showed moderately fluctuating baselines, caused by slight admixture of fundamental Raman spectrum due to intensity drifts or sample reinsertion inaccuracies. This introduced fluctuations in spectral positions of several peaks in the difference spectrum, marked by "*" in Figure 5. In contrast, the spectral positions of 3 peaks

DOI: 10.1021/acs.jpcc.6b13095
J. Phys. Chem. C 2017, 121, 5261−5266

located at 546.2, 953.5, and 1549.6 cm^{-1} were not significantly affected by these inaccuracies and may be considered as reliable.

DISCUSSION

Luminescence of Cl_2. A comparison of the characteristic shape of the PL emission band in Figure 1 with the triplet-to-singlet a $^3\Pi_u \rightarrow X\ ^1\Sigma_g^+$ emission reported for matrix-isolated Cl_2 molecules in Ar, Kr, and Xe cryo-crystals[13,17,18] leaves little doubt that the "1.22 eV" PL band is due to interstitial Cl_2 molecules in SiO_2. This assignment is further corroborated by similar, milliseconds-range PL lifetimes: between 3 to 15 ms in our work (Figure 4) and 83, 76, and 55 ms in Ne, Ar and Kr cryocrystals, respectively.[17] The vibronic lines of Cl_2 PL in Ar crystals are much sharper than in a-SiO_2, and separate vibronic progressions for three different naturally occurring isotopic compositions of Cl_2: $^{35}Cl-^{35}Cl$ (57.4%), $^{35}Cl-^{37}Cl$ (36.7%), and $^{37}Cl-^{37}Cl$ (5.9%) are observed.[13] If the positions of "isotope-averaged" vibronic PL lines of Cl_2 in Ar are calculated as weighed average of the reported[13] vibronic line positions of these 3 Cl_2 isotopologues, then they coincide with those of the vibronic peaks between 1.9 and 1.3 eV in Figure 1 very well. The deviations (4 meV) were less than the spectral resolution (5 meV). The separations of adjacent vibronic peaks in Figure 1 decrease linearly with the quantum number, with a slope of (0.76 ± 0.06) meV (6.2 ± 0.5 cm^{-1}), which yields the anharmonicity parameter $\omega\chi$ = (3.1 ± 0.25) cm^{-1} in the standard Morse potential model describing the dependence of emission energy $E(v)$ on excited state zero-phonon ($v' = 0$) energy E_0, ground state vibrational quantum number v, harmonic vibrational frequency ω (in cm^{-1} units), and anharmonicity parameter $\omega\chi$:

$$E(v) = E_0 - hc\left[\omega\left(v + \frac{1}{2}\right) - \omega\chi\left(v + \frac{1}{2}\right)^2\right] \quad (1)$$

This $\omega\chi$ value (3.1 cm^{-1}) is close to its reported values for Cl_2 in Ar (2.73 cm^{-1}) or Kr (2.77 cm^{-1}) matrices.[17] $E(0) - E(1)$ is given independently by 546.2 cm^{-1} Cl_2 line in the Raman spectrum (see below). Then the harmonic frequency ω = 546.2 cm^{-1} + 2$\omega\chi$ = 552.4 cm^{-1}, and the PL spectrum is best fitted with E_0 = 17008 cm^{-1}. This predicts "isotope-weighted" zero-phonon transition energy ≈2.074 eV and allows an assignment of vibrational numbers v to the subbands in PL spectrum (Figure 1). It coincides with the v assignments made for PL bands of Cl_2 in the Ar matrix.[13,17]

The peak position (3.78 eV) and fwhm (0.67 eV) of the absorption band (Figure 2A) coincide well with those reported previously for Cl_2 in SiO_2[1] and for free Cl_2 molecules (3.762 and 0.68 eV, respectively).[7] The PLE spectrum nearly exactly coincides with the absorption spectrum, the slightly smaller half-width (≈0.6 eV) can be attributed to the difference between the measurement temperatures of PLE (T = 14 K) and OA (T = 295 K) spectra. As far as we know, a-SiO_2 is the only oxide material for which matrix-isolated luminescence of Cl_2 has been reported. The intensity of the PL in our sample with 7 × 10^{17} Cl_2/cm^3 allows one to estimate that <10^{14} Cl_2/cm^3 in mm-sized samples and <10^{12} Cl_2/cm^3 in optical fibers could be easily detected.

The 3.78 eV OA and PLE band of Cl_2 is due to the transition from the ground state $X\ ^1\Sigma_g^+$ to A $^1\Pi_u$. The emission occurs from the lowest triplet state a $^3\Pi_u$. The potential energy curves calculated for these states[15] and absorption-emission transitions observed in the present work are shown in Figure 2, inset. A more detailed term scheme, which takes into account the spin–orbital coupling in $^3\Pi_u$ state, is calculated in ref 19.

In a free Cl_2 molecule, the $^1\Pi_u$ excited state is repulsive, with energy above the dissociation energy (2.5 eV) (Figure 2, see ref 20 for an overview of Cl_2 properties). Evidently, in a-SiO_2 matrix, the Cl atoms are held together by the "cage effect" and PL occurs after relaxation to the lowest triplet manifold $^3\Pi_u$. For Cl_2 in inert gas crystals, the cage effect is very strong in Ar, smaller in Kr, and weak in Xe cryocrystals.[21,22] While Cl_2 in Xe is dissociated by excitation in the 3.78 eV OA band,[21] in the case of Ar matrix the threshold of efficient dissociation is 9.2 eV with a weaker threshold at 6.2 eV.[22] The decrease of cage effect in the row of Ar → Kr → Xe crystals correlates with an increase of the respective lattice constants (526, 571, and 620 pm, respectively) of their fcc cubic structures.

In the case of a-SiO_2, photobleaching of Cl_2 PL was not observed at any excitation photon energy within the 2.33–4.66 eV range, used in this study. Taking into account the power density of the focused laser beam, the irradiation duration and the published[7] Cl_2 absorption cross section, we estimated that the permanent dissociation probability of Cl_2 molecule on absorbing of 4.66 eV photon was <1% at T = 13 K. The average diameter of interstitial voids in the structure of a-SiO_2 is around 400–500 pm, as estimated from positron annihilation[23] or reverse Monte Carlo simulation studies.[24] The largest sites may accommodate a Cl_2 molecule (Cl–Cl distance, 199 pm; transversal van der Waals diameter, 380 pm[25]). The absence of photobleaching indicates that neighboring sites, appropriate for stabilizing the separated Cl atom, are not easily reached. Neutral interstitial Cl atoms (Cl^0) have been detected by electron paramagnetic resonance in Cl-containing a-SiO_2 only after a much higher energy (100 keV X-rays) excitation.[26] It is suggested that Cl^0 is responsible for absorption bands in X-ray irradiated SiO_2-core optical fibers at 3.5 eV[27] and for γ-ray-induced absorption of optical fibers in the near-infrared region.[2,28]

The optical absorption cross section spectrum[7] and calculations[15,19] indicate that absorption at photon energies <2.5 eV is due to the spin-forbidden $X\ ^1\Sigma_g^+ \rightarrow$ a $^3\Pi_u$ transition (Figure 2, inset). The weak PL of interstitial Cl_2 in a-SiO_2, detected under 2.33 eV laser light (Figure 3), evidently is excited via this transition.

Raman Signals of Cl_2 and ClClO. Out of the three reliably measured Raman peaks, marked by arrows in difference spectrum in Figure 5, the peak at 1549.6 cm^{-1} is easily identified as due to interstitial O_2 molecules in SiO_2. Its closeness to the exactly measured value of 1548.5 cm^{-1}[29] gives an additional confidence that positions of the other two, unassigned peaks are accurate within ±1 cm^{-1}. The strongest of them, located at 546.2 cm^{-1}, can be assigned to an interstitial Cl_2 in a-SiO_2 because: (i) it is larger in the sample S2 with larger Cl_2 concentration (Table 1), and (ii) its position is very close to (v = 0) → (v = 1) energy for the $^{35}Cl-^{35}Cl$ in gas (554.3 cm^{-1}) or in Ar matrix (549.2 cm^{-1}).[17] Additionally, as discussed above, using this Raman band energy in Morse-potential vibrational energy calculation eq 1 yields the same assignments of vibrational quantum numbers as for Cl_2 in Ar matrix.

The sharp Raman peak at 953.5 cm^{-1} in difference spectrum (Figure 5) has not been previously reported in SiO_2. It is likely related to the difference in Cl concentrations in samples S2 and S0. Similar peak in UV resonance Raman spectra at 954 cm^{-1} has been assigned to Cl–O stretch in ClClO molecules

DOI: 10.1021/acs.jpcc.6b13095
J. Phys. Chem. C 2017, 121, 5261–5266

dissolved in CCl_4.[30] ClClO molecules in Ar matrix give rise to IR absorption bands at 961.7 cm^{-1} (Cl−^{35}Cl−O) or 953.4 cm^{-1} (Cl−^{37}Cl−O).[31] On the other hand, it is well-known that O_2 in a-SiO_2 is less constrained by cage-effect, and that F_2-laser photolysis creates mobile O atoms.[32] Evidently, a reaction

$$Cl_2 + O \rightarrow ClClO \quad (2)$$

takes place. Dichlorine monoxide is the largest interstitial 3 atom species detected until now in a-SiO_2: interstitial ozone O_3,[32] water H_2O, hydroperoxy radical HO_2[33] and chlorine dioxide ClO_2,[34] only 4-atom chlorate radical ClO_3[34] is larger. Our present Raman data (Figure 5) do not confirm a creation of another isomer of dichlorine monoxide, Cl−O−Cl. It should show Raman band due to the symmetric stretch mode around 640 cm^{-1};[31,35] however, the 640 cm^{-1} peak, marked by an asterisk in Figure 5, was not consistently present in all difference spectra (Results), and thus cannot be confirmed on the basis of the present data.

The formation of dichlorine monoxide in a-SiO_2 may be of practical importance. Reaction 2 may deplete the concentration of interstitial O_2 in O_2-loaded a-SiO_2 optical fibers, suggested as radioluminescent detectors for dosimetric applications.[36] The creation of ClClO can strongly affect optical elements and fibers for UV region, where a-SiO_2 is the usual material of choice. The OA cross section σ of ClClO is large (1.3×10^{-17} cm^2 at 260 nm[31]); it is ≈100 times larger than σ for the UV OA band of free Cl_2 molecule.[7] Therefore, the formation of ClClO may be an important and so far not considered mechanism contributing to the well-known detrimental effect of chlorine impurities on UV optical transmission of a-SiO_2.

CONCLUSIONS

With the proliferation of near-infrared-sensitive Si detectors, the luminescence of interstitial Cl_2 molecules in amorphous SiO_2 has become easy to observe. It provides sensitive and highly specific spectral signature, suitable for monitoring of molecular chlorine, and its chemical and photoinduced reactions in amorphous SiO_2. In this work, detailed characteristics of this luminescence were obtained. Additionally, the Raman signal of Cl_2 in SiO_2 was observed for the first time. Cl_2 molecule in amorphous SiO_2 is stabilized by a strong cage effect, preventing its photodissociation by photons with energy <5 eV. However, Cl_2 can accept in its cage an additional atomic oxygen created by photolysis of interstitial O_2 and form ClClO molecule. This molecule is a strong ultraviolet absorber and suppression of its formation may be important for irradiation- and solarization-resistant SiO_2-based UV optics.

AUTHOR INFORMATION

Corresponding Author

*(L.S.) E-mail skuja@latnet.lv.

ORCID

Linards Skuja: 0000-0001-7918-900X

Notes

The authors declare no competing financial interest.

ACKNOWLEDGMENTS

The support from the Latvian Research Program project IMIS 2 (L.S., K.S.) and Latvian Science Council Grant 302/2012 (A.S.) is acknowledged. K.K. was partially supported by the Collaborative Research Project of Materials and Structures Laboratory, Tokyo Institute of Technology. H.H. was supported by the MEXT Element Strategy Initiative to form research cores.

REFERENCES

(1) Awazu, K.; Kawazoe, H.; Muta, K.; Ibuki, T.; Tabayashi, K.; Shobatake, K. Characterization of Silica Glasses, Sintered Under Cl_2 Ambients. *J. Appl. Phys.* **1991**, *69*, 1849−1852.

(2) Girard, S.; Kuhnhenn, J.; Gusarov, A.; Brichard, B.; Van Uffelen, M.; Ouerdane, Y.; Boukenter, A.; Marcandella, C. Radiation Effects on Silica-Based Optical Fibers: Recent Advances and Future Challenges. *IEEE Trans. Nucl. Sci.* **2013**, *60*, 2015−2036.

(3) Chiodini, N.; Lauria, A.; Lorenzi, R.; Brovelli, S.; Meinardi, F.; Paleari, A. Sol−Gel Strategy for Self-Induced Fluorination and Dehydration of Silica with Extended Vacuum Ultraviolet Transmittance and Radiation Hardness. *Chem. Mater.* **2012**, *24*, 677−681.

(4) Rosplock, C. K.; Sempolinski, D. R. Fused Silica Lens, Microlithography System Including a Fused Silica Lens and Method of Making a Fused Silica Lens. U.S. Patent 5,896,222, April 20, 1999.

(5) Kajihara, K.; Hirano, M.; Skuja, L.; Hosono, H. Reactions of SiCl groups in Amorphous SiO_2 With Mobile Interstitial Chemical Species: Formation of Interstitial Cl_2 and HCl Molecules, and Role of Interstitial H_2O Molecules. *J. Appl. Phys.* **2005**, *98* (4), 043515.

(6) Takei, T.; Kato, K.; Meguro, A.; Chikazawa, M. Infrared Spectra of Geminal and Novel Triple Hydroxyl Groups on Silica Surface. *Colloids Surf., A* **1999**, *150*, 77−84.

(7) Maric, D.; Burrows, J. P.; Meller, R.; Moortgat, G. K. A Study of the UV-Visible Absorption Spectrum of Molecular Chlorine. *J. Photochem. Photobiol., A* **1993**, *70*, 205−214.

(8) Skuja, L.; Kajihara, K.; Hirano, M.; Hosono, H. Visible to Vacuum-UV Range Optical Absorption of Oxygen Dangling Bonds in Amorphous SiO_2. *Phys. Rev. B: Condens. Matter Mater. Phys.* **2011**, *84* (20), 205206.

(9) Skuja, L. Isoelectronic Series of Twofold Coordinated Si, Ge, and Sn Atoms in Glassy SiO_2: a Luminescence Study. *J. Non-Cryst. Solids* **1992**, *149*, 77−95.

(10) Sakurai, Y.; Nagasawa, K. Correlation Between the 1.5 eV Photoluminescence-Band and the 3.8 eV Absorption Band in Silica Glass. *J. Non-Cryst. Solids* **2000**, *261*, 21−27.

(11) Sakurai, Y. Correlation Between the 1.5 eV Photoluminescence Band and Peroxy Linkage in Silica Glass. *J. Non-Cryst. Solids* **2000**, *276*, 159−162.

(12) Skuja, L. Optical Properties of Defects in Silica. In *Defects in SiO_2 and Related Dielectrics: Science and Technology*; Pacchioni, G., Skuja, L., Griscom, D. L., Eds.; NATO Science Series II, Kluwer: Dordrecht, The Netherlands, Boston, MA, and London, 2000; Vol. 2, pp 73−116.

(13) Ault, B. S.; Howard, W. F., Jr.; Andrews, L. Laser-Induced Fluorescence and Raman Spectra of Chlorine and Bromine Molecules Isolated in Inert Matrices. *J. Mol. Spectrosc.* **1975**, *55*, 217−228.

(14) Zeng, Q.; Stebbins, J. F.; Heaney, A. D.; Erdogan, T. Hydrogen Speciation in Hydrogen-Loaded, Germania-Doped Silica Glass: a Combined NMR and FTIR Study of the Effects of UV Irradiation and Heat Treatment. *J. Non-Cryst. Solids* **1999**, *258*, 78−91.

(15) Peyerimhoff, S. D.; Buenker, R. J. Electronically Excited and Ionized States of the Chlorine Molecule. *Chem. Phys.* **1981**, *57*, 279−296.

(16) Skuja, L.; Kajihara, K.; Hirano, M.; Hosono, H. Oxygen-Excess-Related Point Defects in Glassy/Amorphous SiO_2 and Related Materials. *Nucl. Instrum. Methods Phys. Res., Sect. B* **2012**, *286*, 159−168.

(17) Bondybey, V. E.; Fletcher, C. Photophysics of Low Lying Electronic States of Cl_2 in Rare Gas Solids. *J. Chem. Phys.* **1976**, *64*, 3615−3620.

(18) McCaffrey, J. G.; Kunz, H.; Schwentner, N. Spectroscopy and Photodissociation of Chlorine Monomers and Clusters in Argon Matrices. *J. Chem. Phys.* **1992**, *96*, 155−164.

(19) Asano, Y.; Yabushita, S. Theoretical Study on the Nonadiabatic Transitions in the Photodissociation Processes of Cl_2. *J. Phys. Chem. A* **2001**, *105*, 9873−9882.

DOI: 10.1021/acs.jpcc.6b13095
J. Phys. Chem. C 2017, 121, 5261−5266

(20) Christophorou, L. G.; Olthoff, J. K. Electron Interactions with Cl_2. *J. Phys. Chem. Ref. Data* **1999**, *28*, 131−169.
(21) McCaffrey, J. G.; Kunz, H.; Schwentner, N. Photodissociation of Molecular Chlorine in Xenon Matrices. *J. Chem. Phys.* **1992**, *96*, 2825−2833.
(22) Kunz, H.; McCaffrey, J. G.; Schriever, R.; Schwentner, N. Spectroscopy and Photodissociation of Molecular Chlorine in Argon Matrices. *J. Chem. Phys.* **1991**, *94*, 1039−1045.
(23) Zanatta, M.; Baldi, G.; Brusa, R. S.; Egger, W.; Fontana, A.; Gilioli, E.; Mariazzi, S.; Monaco, G.; Ravelli, L.; Sacchetti, F. Structural Evolution and Medium Range Order in Permanently Densified Vitreous SiO_2. *Phys. Rev. Lett.* **2014**, *112* (4), 045501.
(24) Kohara, S.; Akola, J.; Morita, H.; Suzuya, K.; Weber, J. K. R.; Wilding, M. C.; Benmore, C. J. Relationship Between Topological Order and Glass Forming Ability in Densely Packed Enstatite and Forsterite Composition Glasses. *Proc. Natl. Acad. Sci. U. S. A.* **2011**, *108*, 14780−14785.
(25) Batsanov, S. S. Van der Waals Radii of Elements. *Inorg. Mater.* **2001**, *37*, 871−885.
(26) Griscom, D. L.; Friebele, E. J. Fundamental Radiation-Induced Defect Centers in Synthetic Fused Silicas: Atomic Chlorine, Delocalized E′ Centers, and a Triplet State. *Phys. Rev. B: Condens. Matter Mater. Phys.* **1986**, *34*, 7524−7533.
(27) Girard, S.; Ouerdane, Y.; Origlio, G.; Marcandella, C.; Boukenter, A.; Richard, N.; Baggio, J.; Paillet, P.; Cannas, M.; Bisutti, J.; et al. Radiation Effects on Silica-Based Preforms and Optical Fibers - I: Experimental Study With Canonical Samples. *IEEE Trans. Nucl. Sci.* **2008**, *55*, 3473−3482.
(28) Tomashuk, A. L.; Salgansky, M.; Kashaykin, P.; Khopin, V.; Sultangulova, A.; Nishchev, K.; Borisovsky, S.; Guryanov, A.; Dianov, E. Enhanced Radiation Resistance of Silica Optical Fibers Fabricated in High O_2 Excess Conditions. *J. Lightwave Technol.* **2014**, *32*, 213−219.
(29) Skuja, L.; Güttler, B.; Schiel, D.; Silin, A. R. Quantitative Analysis of the Concentration of Interstitial O_2 Molecules in SiO_2 Glass Using Luminescence and Raman Spectrometry. *J. Appl. Phys.* **1998**, *83*, 6106−6110.
(30) Esposito, A. P.; Reid, P. J.; Rousslang, K. W. A Resonance Raman Study of Cl_2O Photochemistry in Solution: Evidence for ClClO Formation. *J. Photochem. Photobiol., A* **1999**, *129*, 9−15.
(31) Johnsson, K.; Engdahl, A.; Nelander, B. The UV and IR spectra of the ClClO Molecule. *J. Phys. Chem.* **1995**, *99*, 3965−3968.
(32) Kajihara, K.; Skuja, L.; Hosono, H. Diffusion and Reactions of Photoinduced Interstitial Oxygen Atoms in Amorphous SiO_2 Impregnated with ^{18}O-Labeled Interstitial Oxygen Molecules. *J. Phys. Chem. C* **2014**, *118*, 4282−4286.
(33) Kajihara, K.; Hirano, M.; Skuja, L.; Hosono, H. Role of Interstitial Voids in Oxides on Formation and Stabilization of Reactive Radicals: Interstitial HO_2 Radicals in F_2 -Laser-Irradiated Amorphous SiO_2. *J. Am. Chem. Soc.* **2006**, *128*, 5371−5374.
(34) Nishikawa, H.; Nakamura, R.; Ohki, Y.; Nagasawa, K.; Hama, Y. Characterization of ClO_x Radicals in Vacuum-Ultraviolet-Irradiated High-Purity Silica Glass. *Phys. Rev. B: Condens. Matter Mater. Phys.* **1992**, *46*, 8073−8079.
(35) Beltrán, A.; Andrés, J.; Noury, S.; Silvi, B. Structure and Bonding of Chlorine Oxides and Peroxides: ClO_x, ClO_x^- (x = 1−4), and Cl_2O_x (x = 1−8). *J. Phys. Chem. A* **1999**, *103*, 3078−3088.
(36) Di Francesca, D.; Girard, S.; Agnello, S.; Marcandella, C.; Paillet, P.; Boukenter, A.; Gelardi, F. M.; Ouerdane, Y. Near Infrared Radio-Luminescence of O_2 Loaded Radiation Hardened Silica Optical Fibers: A Candidate Dosimeter for Harsh Environments. *Appl. Phys. Lett.* **2014**, *105* (18), 183508.

DOI: 10.1021/acs.jpcc.6b13095
J. Phys. Chem. C 2017, 121, 5261−5266